J. Fluid Mech. (1992), *vol.* 239, *pp.* 249–271
Printed in Great Britain

Analysis of a rapidly rotating gas in a pie-shaped cylinder

By HOUSTON G. WOOD[1] AND RICHARD BABARSKY[2]

[1]Mechanical and Aerospace Engineering, University of Virginia, Charlottesville, VA 22901, USA

[2]Mathematics and Computer Science, James Madison University, Harrisonburg, VA 22801, USA

(Received 27 April 1990 and in revised form 5 November 1991)

By using asymptotic analysis, an eigensolution technique has been developed for predicting the flow of gas contained in a pie-shaped cylinder of finite length rotating rapidly about its vertex. This problem has application to a conventional cylindrical gas centrifuge with radial walls. Three different types of boundary layers exist in the flow: Ekman layers on the top and bottom, buoyancy layers on the radial walls, and a cylindrical 'pancake' layer on the outer wall of the cylinder. A single sixth-order partial differential equation is obtained for the axial velocity in the cylindrical layer, and the other layers provide matching conditions. The problem is formulated for no-slip and prescribed temperature conditions on the solid surfaces and for adiabatic no shear stress with zero pressure at the inner free surface. Eigenvalues are computed for this problem and compared with those for the open cylinder, and solutions are presented for flows induced by mass throughput and by differential temperature conditions.

1. Introduction

The dynamics of rapidly rotating gases have been investigated by numerous authors with the primary application to gas centrifuges for the enrichment of fissionable isotopes of uranium. Such investigations have been reported by Sakurai & Matsuda (1974), Rätz (1978), Soubbaramayer (1979), and Wood & Morton (1980). In these investigations the gas centrifuge was treated as an open cylinder and the resulting flow field was considered to be axisymmetric. Matsuda & Nakagawa (1983) reported an investigation of a non-axisymmetric flow field which arises for a sectored cylinder with radial walls. These walls confine the gas to a pie-shaped region which is rotating about its apex (see figure 1). In their analysis, Matsuda & Nakagawa, who considered the case of an infinitely long cylinder in which the atmospheric scale height is of the order of the bowl radius, identified a new type of boundary layer, called a buoyancy layer, that exists along the radial walls and is of order $E^{\frac{1}{4}}$, where E is the Ekman number.

In this paper we relax the restrictions imposed by Matsuda & Nakagawa and consider a pie-shaped cylinder of finite length in which the density scale height is small compared to the radius. A formal asymptotic method is used to develop an approximate model for the flow in this case of high rotational speed. This approximate model can be described in terms of a non-symmetric potential, χ, by the following equation

$$(\mathrm{e}^x(\mathrm{e}^x\chi_{xx})_{xx})_{xx}+2\mathscr{R}^2\mathscr{G}\chi_{\theta\theta}+2\mathscr{R}^2(2+\mathscr{G})\chi_{zz}-2\mathscr{R}\,\mathrm{e}^x\chi_{xx\theta}=0, \tag{1.1}$$

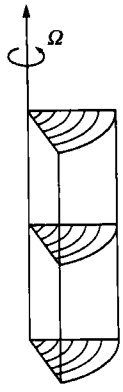

FIGURE 1. Pie-shaped cylinder rotating about the vertex.

where $\mathscr{R}$ and $\mathscr{G}$ are similarity parameters and x, θ, and z are the radial, azimuthal and axial coordinates respectively. In the case of moderate rotational speed in which the atmospheric scale height is of order of the cylinder radius, the cross-derivative term may be neglected and the resulting model is the same as that obtained by Matsuda & Nakagawa. In the case of axial symmetry, the terms which exhibit azimuthal variation vanish and the model yields Onsager's 'pancake' equation (see Wood & Morton 1980). (Lars Onsager coined the phrase 'pancake' to describe the high-speed approximation to flow in a centrifuge. He observed that in the limit of high rotation rate, the gas is compressed into a very thin layer near the wall, and hence the algebraic curvature terms may be neglected. The resulting 'atmosphere' within the centrifuge therefore is taken to be 'flat as a pancake'.)

To model accurately a rapidly rotating gas in a pie-shaped cylinder, however, the cross-derivative term is essential and furthermore its presence leads to significant difficulty in obtaining a solution. In the analysis presented herein, a Galerkin-type method is employed and the expansion functions are derived from the symmetric 'pancake' solution. The symmetric problem leads to a self-adjoint eigenvalue problem, a property which is not preserved in the non-symmetric case. However, it has been shown (Babarsky & Wood 1986) that this non-self adjoint problem does admit eigenvalues and eigenfunctions. A comparison of the eigenvalues of the two problems confirms that the axial decay of the amplitude of flow variables is significantly magnified in the non-symmetric case.

2. Linearized Navier-Stokes equations

2.1. *Reference solution*

Let (r, θ, z) denote cylindrical coordinates with the origin fixed at the bottom of the cylinder (which we take to be a right pie-shaped cylinder) on the axis of rotation. The z-axis lies along the axis of rotation, and the pie-shaped cylinder is restricted by the five walls: $\theta = 0$, $\theta = \theta_0$, $r = a$, $z = 0$ and $z = z_T$. (Note that θ_0, measured in radians, is taken to be order unity.)

For a fluid rotating as a solid body about its axis with frequency Ω the radial, azimuthal, and axial velocity components are given by

$$U = 0, \quad V = \Omega r, \quad W = 0.$$

with the pressure distribution governed by the hydrostatic equation

$$\frac{\mathrm{d}p}{\mathrm{d}r} = \rho\Omega^2 r,$$

where p is the pressure and ρ is the density.

For a perfect gas at uniform temperature T_0 the pressure and density distributions in the cylinder are

$$p = p_{\mathrm{w}} \exp\{-A^2[1-(r/a)^2]\}, \quad \rho = \rho_{\mathrm{w}} \exp\{-A^2[1-(r/a)^2]\},$$

where $A^2 = (\Omega a)^2/(2RT_0)$, p_{w} is the pressure at the outer wall, ρ_{w} is the density at the outer wall, a is the radius of the cylinder, and R is the specific gas constant.

2.2. *Linearized equations*

The equations of motion are made dimensionless by using Ωa, p_{w}, ρ_{w}, T_0, and a for scaling the velocity, pressure, density, temperature, and lengths, respectively. Linearizing the steady (in the rotor-fixed frame) equations about isothermal solid-body rotation yields.

$$(\rho_0 ru)_r + \rho_0 rv_\theta + r\rho_0 w_z = 0, \tag{2.1}$$

$$-r(2\rho_0 v + \rho) = -(1/2A^2)\, p_r + E\{\Delta u - (u/r^2) - \tfrac{2}{3}A^2(ru)_r - 2v_\theta/r\}, \tag{2.2}$$

$$2\rho_0 u = -(1/2A^2 r)\, p_\theta + E\{\Delta(rv) - (v/r) + (1/3r)\,[v_\theta + u_r + (7u/r) + w_z]_\theta\}, \tag{2.3}$$

$$0 = -(1/2A^2)\, p_z + E\{\Delta w - \tfrac{2}{3}A^2 r u_z\}, \tag{2.4}$$

$$0 = 2\Gamma\rho_0 ru + E\Delta T, \tag{2.5}$$

$$p = \rho_0 T + \rho, \tag{2.6}$$

where $E = \mu/\rho_{\mathrm{w}}\Omega a^2$, $Pr = \mu c_p/k$, $\Gamma = A^2 Pr(\gamma-1)/\gamma$, $\gamma = c_p/c_v$,

and $$\rho_0 = p_0 = \exp\{-A^2(1-r^2)\}.$$

Here we have assumed that the specific heats, viscosity, and thermal conductivity are functions of temperature only.

It should be noted that (2.1)–(2.6) differ from those derived by Schleiniger & Cole (1982) who also studied non-axisymmetric flow in a gas centrifuge. The differences derive from the nature of the disturbances they considered, which are non-axisymmetric but steady with respect to the laboratory frame. This is in contradistinction to the case at hand in which we consider flows which are steady in the rotating frame.

3. Pancake theory

3.1. *The asymptotic limit* $\delta \to 0$

Following Schleineger & Cole (1982) we develop a high-speed limit approximation to obtain a non-axisymmetric pancake theory. We observe the dependence of the governing equations upon three parameters ; the speed parameter A^2, the peripheral Ekman number E, and the compressibility parameter, Γ (which contains the factor $A^2(\gamma-1)/\gamma$).

For operating conditions characteristic of high-speed centrifuges we anticipate that A shall be large and E small. Thus, in the limit of high rotational speeds we may assume that $A^2 \gg 1$ (note $1/2A^2$ is equal to the density scale height measured at the

outer radius) so that essentially all the gas is confined to a thin layer near the outer radial boundary. In this 'pancake layer' we anticipate a balance between stratification effects associated with high-speeds and viscous effects (radial diffusion). Taking $1/2A^2$ as the basic small parameter we let

$$\delta = 1/2A^2 \to 0,$$

with the limit process characterized by $\delta \to 0$, $E \to 0$ and $\gamma \to 1$ (we shall be considering a polyatomic gas).

In order to resolve stratification effects we keep (x, θ, z) fixed where

$$x = (1-r)/\delta.$$

Now

$$A^2(1-r^2) = A^2(1-r)(1+r) = A^2(1-r)[2-(1-r)] = x - \tfrac{1}{2}\delta x^2.$$

Thus, it can be shown that $\rho_0 = \exp\{-x\} + O(\delta)$. In other words, x measures the distance from the outer wall of the cylinder in scale heights.

For a polyatomic gas a characteristic feature of compressible motion in a strong centrifugal field is the coupling between the velocity and temperature which is due to the work done by the pressure as the fluid particle appreciably swells or shrinks during radial motion. Therefore, the parameter Γ plays a decisive role in high-speed gas centrifuge flows.

It follows then that in order to maintain the balance of relevant forces in the pancake layer the following similarity parameters are obtained (see Wood & Babarsky 1987):

$$\mathscr{R} = \delta^3/E \quad \text{and} \quad \mathscr{G} = \Gamma,$$

where these parameters indicate the rate at which $E \to 0$ and $\gamma \to 1$ relative to $\delta \to 0$.

3.2. *The equations of the pancake layer*

The resulting asymptotic expansion in the pancake layer far from the axial and azimuthal boundaries (where axial and azimuthal diffusion must be considered) may then be shown to be

$$\begin{aligned}
u(r,\theta,z;A^2,E,\Gamma) &= \delta u^*(x,\theta,z;\mathscr{R},\mathscr{G}) + \ldots,\\
v(r,\theta,z;A^2,E,\Gamma) &= v^*(x,\theta,z;\mathscr{R},\mathscr{G}) + \ldots,\\
w(r,\theta,z;A^2,E,\Gamma) &= w^*(x,\theta,z;\mathscr{R},\mathscr{G}) + \ldots,\\
p(r,\theta,z;A^2,E,\Gamma) &= p^*(x,\theta,z;\mathscr{R},\mathscr{G}) + \ldots,\\
\rho(r,\theta,z;A^2,E,\Gamma) &= \rho^*(x,\theta,z;\mathscr{R},\mathscr{G}) + \ldots,\\
T(r,\theta,z;A^2,E,\Gamma) &= T^*(x,\theta,z;\mathscr{R},\mathscr{G}) + \ldots.
\end{aligned}$$

We note that only the radial velocity is asymptotically small. The resulting system constitutes the 'pancake' approximation for non-axisymmetric flow in a gas centrifuge:

$$-(\rho_0 u^*)_x + \rho_0 v^*_\theta + \rho_0 w^*_z = 0, \tag{3.1}$$

$$2\rho_0 v^* + \rho^* = -p^*_x, \tag{3.2}$$

$$2\rho_0 u^* = -p^*_\theta + (1/\mathscr{R})\, v^*_{xx}, \tag{3.3}$$

$$p^*_z = (1/\mathscr{R})\, w^*_{xx}, \tag{3.4}$$

$$2\mathscr{G}\rho_0 u^* = -(1/\mathscr{R})\, T^*_{xx}, \tag{3.5}$$

$$p^* = \rho^* + \rho_0 T^*. \tag{3.6}$$

We see from the above equations that in the non-axisymmetric pancake layer explicit θ-dependence is reflected in a three-dimensional mass conservation equation and in the presence of an azimuthal pressure gradient which counteracts the balance between the Coriolis force and azimuthal shear.

Now following Maslen's (1984) development, we define two quantities which are relevant to rotating compressible flows:

$$\varphi^* = T^* - 2v^* \quad \text{and} \quad H^* = T^* + \mathscr{G}v^*.$$

The approximate model may then be described by the following system of equations:

$$-(\rho_0 u^*)_x + \rho_0 v^*_\theta + \rho_0 w^*_z = 0, \tag{3.7}$$

$$\varphi^* = (p^*/\rho_0)_x, \tag{3.8}$$

$$\varphi^*_{xx} = -2\mathscr{R}p^*_\theta - 2\mathscr{R}\rho_0(2+\mathscr{G})\,u^*, \tag{3.9}$$

$$p^*_z = (1/\mathscr{R})\,w^*_{xx}, \tag{3.10}$$

$$H^*_{xx} = \mathscr{R}\mathscr{G}p^*_\theta. \tag{3.11}$$

We shall now consider typical boundary conditions for end-driven flows. At the rotor wall we require that the radial, axial, and azimuthal velocities and perturbation temperature vanish (i.e. $u = w = v = T = 0$). As noted above, in the asymptotic limit ($\delta \to 0$), to order δ, $u = 0$. Hence, to the level of approximation of this analysis (all quantities represent highest-order terms in an asymptotic expansion in terms of δ), the normal flow condition is identically satisfied. However, to be consistent with the usual interpretation of the $O(1)$ problem as the first in an infinite sequence of problems consisting of partial differential equations and accompanying boundary condition, we shall impose the following conditions at the $x = 0$ boundary:

$$u^* = w^* = v^* = T^* = 0, \tag{3.12}$$

which also implies

$$\varphi^* = 0. \tag{3.13}$$

At the inner boundary of the region over which the continuum equations are valid, $x = x_T$, we impose the boundary conditions

$$w^*_x = v^*_x = T^*_x = p^* = 0, \tag{3.14}$$

which also implies $\varphi^*_x = 0$ and where these conditions (note that the first three quantities represent lower-order terms in the expressions for the corresponding shear stresses and radial temperature gradient) are consistent with the class of conditions that are expected to prevail in this low-density regime (see Cooper & Morton 1988).

The appropriate conditions to be imposed at the axial and azimuthal boundaries are provided by matching with the solutions to the Ekman-layer and buoyancy-layer equations.

4. The compressible Ekman layers

For a rapidly rotating cylinder spinning about its vertical axis, boundary layers form on the horizontal flat surfaces. In these regions of large velocity and temperature gradients the Coriolis forces and expansion–compression work term necessarily vary dramatically. Thus, in order to maintain the balance of these forces with the radial shear and pressure forces, axial diffusion (of momentum and heat) terms become significant. By focusing on the prevailing forces at work we may then formulate a tractable approximate problem.

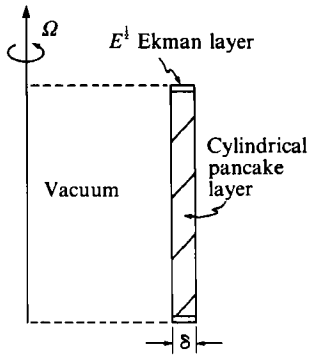

FIGURE 2. Flow field in a rapidly rotating pie-shaped cylinder, (r,z)-plane. $\delta = 1/(2A^2)$ is the radial extent of the flow field.

4.1. *Ekman-layer scaling*

Let us consider the Ekman layer along the $z = 0$ wall. The analysis for the top end is similar. We anticipate the thickness of this layer to be of order $E^{\frac{1}{2}}$. Thus we seek an asymptotic expansion for our solution for which there are terms with argument (x, θ, ζ) fixed (note that the stretched radial variable will remain fixed) in the limit $\delta \to 0$, where

$$\zeta = z/\delta^{\frac{3}{2}}.$$

Thus, as expected, axial diffusion effects are restricted to regions of thickness smaller than that of the radial scale (see figure 2).

In preserving a non-trivial system while balancing the predominate forces known to be acting in this region (i.e. axial diffusion terms balanced by pressure, Coriolis, transport and radial diffusion terms) we consider an asymptotic expansion near $z = 0$ of the form

$$\begin{aligned}
u(r,\theta,z;A^2,E,\Gamma) &= \tilde{u}(x,\theta,\zeta;\mathscr{R},\mathscr{G})+\ldots,\\
v(r,\theta,z;A^2,E,\Gamma) &= \tilde{v}(x,\theta,\zeta;\mathscr{R},\mathscr{G})+\ldots,\\
w(r,\theta,z;A^2,E,\Gamma) &= W_{\mathrm{B}}(x,\theta)+\delta^{\frac{1}{2}}\tilde{w}(x,\theta,\zeta;\mathscr{R},\mathscr{G})+\ldots,\\
p(r,\theta,z;A^2,E,\Gamma) &= \tilde{p}(x,\theta,\zeta;\mathscr{R},\mathscr{G})+\ldots,\\
\rho(r,\theta,z;A^2,E,\Gamma) &= \tilde{\rho}(x,\theta,\zeta;\mathscr{R},\mathscr{G})+\ldots,\\
T(r,\theta,z;A^2,E,\Gamma) &= \tilde{T}(x,\theta,\zeta;\mathscr{R},\mathscr{G})+\ldots,
\end{aligned}$$

where the terms with a tilde must decay like $\mathrm{e}^{-\beta\zeta}$ and the $O(1)$ term must be included in order to satisfy the condition $w = W_{\mathrm{B}}(x,\theta)$ at $z = 0$.

Substitution of this form into (2.1)–(2.6) leads to the following equations which are pertinent to the region $\zeta = O(1)$:

$$-(\rho_0\tilde{u})_x+\rho_0\tilde{w}_\zeta = 0, \tag{4.1}$$

$$-(2\rho_0\tilde{v}+\rho) = \tilde{p}_x+(1/\mathscr{R})\tilde{u}_{\zeta\zeta}, \tag{4.2}$$

$$2\rho_0\tilde{u} = (1/\mathscr{R})\tilde{v}_{\zeta\zeta}, \tag{4.3}$$

$$0 = \tilde{p}_\zeta, \tag{4.4}$$

$$0 = 2\mathscr{G}\rho_0\tilde{u}+(1/\mathscr{R})\tilde{T}_{\zeta\zeta}, \tag{4.5}$$

$$\tilde{p} = \rho_0\tilde{T}+\tilde{\rho}. \tag{4.6}$$

Note that θ appears only parametrically in this system (i.e. the Ekman extension to the pancake layer is essentially axisymmetric).

4.2. *Solution of the approximate equations*

At the bottom boundary the flow should satisfy boundary conditions of the form

$$v = 0, \quad u = 0, \quad w = W_{\mathrm{B}}, \quad T = T_{\mathrm{B}},$$

where W_{B} and T_{B} represent functions of θ and x. As $\zeta \to \infty$ matching conditions must be imposed, which precludes linear growth for the $\tilde{}$ terms. From (4.3) and (4.5) we obtain

$$(\tilde{T} + \mathscr{G}\tilde{v})_{\zeta\zeta} = 0,$$

which for no growth at $\zeta \to \infty$ yields

$$\tilde{T} + \mathscr{G}\tilde{v} = T_{\mathrm{B}} \quad \text{or} \quad \tilde{v} = \frac{1}{\mathscr{G}}(T_{\mathrm{B}} - \tilde{T}).$$

Also from (4.14) we conclude that

$$\tilde{p} = p_{\mathrm{B}}(x, \theta),$$

where $p_{\mathrm{B}}(x, \theta)$ will be determined from matching with the pancake expansion.

After some analysis the solution in the Ekman layer may be shown to be

$$\tilde{u} = -\frac{1}{[2(2+\mathscr{G})^{\frac{1}{2}}}\left[T_{\mathrm{B}} - \left(\frac{p_{\mathrm{B}}}{\rho_0}\right)_x\right] \mathrm{e}^{-\beta_{\mathrm{E}}\zeta} \sin \beta_{\mathrm{E}} \zeta,$$

$$\tilde{v} = \frac{1}{\mathscr{G}+2}\left[T_{\mathrm{B}} - \left(\frac{p_{\mathrm{B}}}{\rho_0}\right)_x\right](1 - \mathrm{e}^{-\beta_{\mathrm{E}}\zeta} \cos \beta_{\mathrm{E}} \zeta),$$

$$\tilde{w} = \frac{\beta_{\mathrm{E}}}{2(2+\mathscr{G})\rho_0 \mathscr{R}}\left\{T_{\mathrm{B}} - \left(\frac{p_{\mathrm{B}}}{\rho_0}\right)_x - T_{\mathrm{B}_x} + \left(\frac{p_{\mathrm{B}}}{\rho_0}\right)_{xx}\right\}(1 - \mathrm{e}^{-\beta_{\mathrm{E}}\zeta}(\sin \beta_{\mathrm{E}} \zeta + \cos \beta_{\mathrm{E}} \zeta)),$$

$$\tilde{T} = T_{\mathrm{B}} - \mathscr{G}\tilde{v}, \quad \tilde{\rho} = -\rho_0 \tilde{T} + \tilde{p}$$

and

$$\tilde{p} = p_{\mathrm{B}}(x, \theta)$$

where

$$\beta_{\mathrm{E}} = [\tfrac{1}{2}\mathscr{R}^2 \rho_0^2 (2+\mathscr{G})]^{\frac{1}{4}}$$

4.3. *Conditions on the inner flow*

The pancake and Ekman-layer expansions are matched by introducing an intermediate variable

$$z_\eta = z^*/\eta(\delta),$$

where

$$\delta^{\frac{3}{5}} \ll \eta(\delta) \ll 1,$$

so that

$$z^* = \eta z_\eta \to 0,$$

and

$$\zeta = \frac{\eta}{\delta^{\frac{3}{5}}} z_\eta \to \infty$$

(where $\delta \to 0$ and z_η is fixed). Using standard arguments (see Kerkorkian & Cole 1981) matching to first order is achieved provided

$$\left.\begin{aligned} p^*(x, \theta, 0) &= p_{\mathrm{B}}(x, \theta), \\ T^*(x, \theta, 0) &= \left[\frac{2}{\mathscr{G}+2} T_{\mathrm{B}}(x, \theta) - \frac{\mathscr{G}}{\mathscr{G}+2}\left(\frac{p_{\mathrm{B}}}{\rho_0}\right)_x\right], \\ w^*(x, \theta, 0) &= W_{\mathrm{B}}(\mathrm{x}, \theta), \quad v^*(x, \theta, 0) = \frac{1}{\mathscr{G}+2}\left[T_{\mathrm{B}} - \left(\frac{p_{\mathrm{B}}}{\rho_0}\right)_x\right]. \end{aligned}\right\} \tag{4.7}$$

Moreover, in terms of φ^* and H^*

$$\varphi^* = (p_B/\rho_0)_x \quad \text{and} \quad H^* = T_B(x,\theta).$$

Note that the first condition follows from (3.8).

We may then obtain a matching condition on u^* by combining (4.7) and (3.9):

$$2\mathscr{R}\rho_0(2+\mathscr{G})\,u^*(x,\theta,0) = -\left(\frac{p_B}{\rho_0}\right)_{xxx} - 2\mathscr{R}p_{B_\theta}.$$

Also, the boundary functions are constrained to satisfy

$$p_{B_\theta} = \frac{1}{\mathscr{R}\mathscr{G}} T_{B_{xx}}$$

subject to the boundary conditions

$$T_B = \left(\frac{p_B}{\rho_0}\right)_x = \left(\frac{p_B}{\rho_0}\right)_{xxx} + 2\mathscr{R}p_{B_\theta} = 0 \quad \text{at} \quad x = 0$$

and

$$T_{Bx} = \left(\frac{p_B}{\rho_0}\right)_{xx} = p_B = 0 \quad \text{at} \quad x = x_T,$$

where conditions (3.12)–(3.14) have been imposed.

5. Analysis of the buoyancy layer

Borrowing a phrase from Matsuda & Nakagawa (1983) we shall call the boundary layers which form on the θ = constant boundaries buoyancy layers. This is certainly an appropriate term, for since the boundary is vertical and normal to the azimuthal direction, the Coriolis terms do not play a significant part in establishing the balance of forces and motions in this layer. The flow is generated through the interaction between the temperature field and the radial velocity via the expansion–compression work term. This direct coupling between the velocity and temperature leads to a boundary-layer structure which vanishes when compressibility is neglected.

5.1. *Buoyancy-layer scaling*

We consider the $\theta = 0$ boundary. The analysis for $\theta = \theta_0$ is similar. Order of magnitude arguments once again lead to the conclusion that the thickness of the buoyancy layer is of order $E^{\frac{1}{5}}$ (see figure 3). Thus our solution expansion includes terms with argument (x,ξ,z) fixed in the limit $\delta \to 0$, where

$$\xi = \theta/\delta^{\frac{3}{2}}.$$

From various physical considerations (retaining a non-trivial continuity equation, balancing azimuthal diffusion terms with pressure and transport terms) we posit an asymptotic expansion near $\theta = 0$ of the following form:

$$\begin{aligned}
u(r,\theta,z;A^2,E,\Gamma) &= \bar{u}(x,\xi,z;\mathscr{R},\mathscr{G}) + \ldots,\\
v(r,\theta,z;A^2,\epsilon,\Gamma) &= \delta^{\frac{1}{2}}\bar{v}(x,\xi,z;\mathscr{R},\mathscr{G}) + \ldots,\\
w(r,\theta,z;A^2,E,\Gamma) &= \bar{w}(x,\xi,z;\mathscr{R},\mathscr{G}) + \ldots,\\
p(r,\theta,z;A^2,E,\Gamma) &= \bar{w}(x,\xi,z;\mathscr{R},\mathscr{G}) + \ldots,\\
\rho(r,\theta,z;A^2,E,\Gamma) &= \bar{\rho}(x,\xi,z;\mathscr{R},\mathscr{G}) + \ldots,\\
T(r,\theta,z;A^2,E,\Gamma) &= \bar{T}(x,\xi,z;\mathscr{R},\mathscr{G}) + \ldots.
\end{aligned}$$

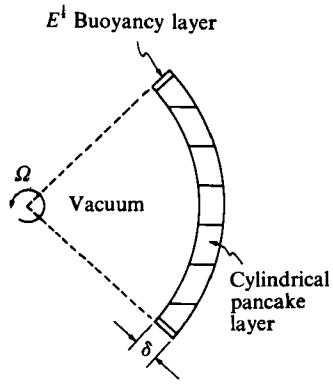

FIGURE 3. Flow field in a rapidly rotating pie-shaped cylinder, (r, θ)-plane.

The appropriate equations in the region $\xi = O(1)$ are then

$$-(\rho_0 \bar{u})_x + \rho_0 \bar{v}_\xi = 0, \tag{5.1}$$

$$-\bar{p} = \bar{p}_x + (1/\mathscr{R})\,\bar{u}_{\xi\xi}, \tag{5.2}$$

$$\bar{p}_\xi = 0, \tag{5.3}$$

$$0 = \bar{w}_{\xi\xi}, \tag{5.4}$$

$$0 = 2\mathscr{G}\rho_0 \bar{u} + (1/\mathscr{R})\,\bar{T}_{\xi\xi}, \tag{5.5}$$

$$\bar{p} = \rho_0 \bar{T} + \bar{\rho}, \tag{5.6}$$

where the axial coordinate appears only parametrically in this system.

Observe that the determination of $\bar{w}$ is decoupled from the boundary-layer problem. Therefore, since solutions to the buoyancy-layer equations must decay exponentially as $\xi \to \infty$ (in order to achieve matching between the buoyancy and pancake layers), equation (5.4) implies that

$$\bar{w} = 0,$$

and hence that the flow in the buoyancy layer is two-dimensional.

In addition, it also follows that

$$\bar{p} = p_{\mathrm{B}}(x, z),$$

where p_{B} is the pressure distribution at the boundary.

5.2. *Solution of the approximate equations*

For the case of impermeable meridional walls the boundary conditions at $\xi = 0$ are

$$\bar{u} = \bar{v} = \bar{w} = 0, \quad \bar{T} = T_{\mathrm{B}}.$$

Substituting (5.6) into (5.2) and using (5.5) yields

$$\bar{u}_{\xi\xi\xi\xi} + 2\mathscr{R}^2\rho_0^2\mathscr{G}\bar{u} = 0$$

so that solutions, in which z and x appear as parameters only, may be written

$$\bar{u} = C\,\mathrm{e}^{-\beta_{\mathrm{B}}\xi}\sin\beta_{\mathrm{B}}\xi, \tag{5.7}$$

where

$$\beta_{\mathrm{B}} = (\tfrac{1}{2}\mathscr{R}^2\rho_0^2\mathscr{G})^{\frac{1}{4}}.$$

Combining (5.2) and (5.6), where $\bar{u}$ is given by (5.7), yields

$$\bar{T} = \left(\frac{p_B}{\rho_0}\right)_x - \left(\frac{2\beta_B^2}{\rho_0 \mathscr{R}}\right) C(x,z)\, e^{-\beta_B \xi} \cos \beta_B \xi.$$

Applying the boundary conditions at $\xi = \frac{1}{2}$ we obtain the following expression for $C(x,z)$:

$$C(x,z) = \frac{1}{(2\mathscr{G})^{\frac{1}{2}}}\left[\left(\frac{p_B}{\rho_0}\right)_x - T_B\right]$$

and hence

$$\bar{u} = \frac{1}{(2\mathscr{G})^{\frac{1}{2}}}\left[\left(\frac{p_B}{\rho_0}\right)_x - T_B\right] e^{-\beta_B \xi} \sin \beta_B \xi$$

and

$$\bar{T} = \left(\frac{p_B}{\rho_0}\right)_x - \left[\left(\frac{p_B}{\rho_0}\right)_x - T_B\right] e^{-\beta_B \xi} \cos \beta_B \xi.$$

Also, combining (5.3) and (5.6) yields

$$\bar{\rho} = -\rho_0 \bar{T} + p_B(x,z).$$

From the continuity equation we have

$$(\rho_0 \bar{u})_x = \rho_0 \bar{v}_\xi,$$

which yields

$$\rho_0 \bar{v} = -\frac{\beta_B}{2\mathscr{G}\rho_0 \mathscr{R}}\left(\rho_0\left[\left(\frac{p_B}{\rho_0}\right)_x - T_B\right]\right)_x (1 - e^{-\beta_B \xi}(\sin \beta_B \xi + \cos \beta_B \xi)),$$

where the appropriate condition on $\bar{v}$ at the boundary has been applied.

Next we consider matching of the buoyancy and pancake layers. To this end, we define an intermediate variable θ_η satisfying

$$\theta_\eta = \frac{\theta^*}{\eta(\delta)},$$

where

$$\delta^{\frac{3}{2}} \ll \eta(\delta) \ll 1,$$

so that matching as

$$z^* = \eta z_\eta \to 0 \quad \text{and} \quad \xi = \frac{\eta}{\delta^{\frac{3}{2}}} z_\eta \to \infty$$

(where $\delta \to 0$ and z_η remains fixed) is achieved to first order provided

$$v^* = 0, \quad w^* = 0, \quad p^* = p_B(x,z), \quad T* = \left(\frac{p_B}{\rho_0}\right)_x.$$

A matching condition on u^* at the $\theta = 0$ boundary may then be obtained from (3.5):

$$2\mathscr{G}\rho_0 u^*(x,0,z) = -\frac{1}{\mathscr{R}}\left(\frac{p_B}{\rho_0}\right)_{xxx},$$

where radial boundary conditions on the pancake variables require that

$$\left(\frac{p_B}{\rho_0}\right)_{xxx} = \left(\frac{p_B}{\rho_0}\right)_x = 0 \quad \text{at} \quad x = 0$$

and $$p_{\mathrm{B}} = \left(\frac{p_{\mathrm{B}}}{\rho_0}\right)_{xx} = 0 \quad \text{at} \quad x = x_{\mathrm{T}}$$

and where (3.10) implies that

$$p_{\mathrm{B}} = p_{\mathrm{B}}(x).$$

6. Axisymmetric solutions in the pancake layer

For the axisymmetric case the pancake system may be reduced to

$$-(\rho_0 u^*)_x + \rho_0 w_z^* = 0, \tag{6.1}$$

$$\varphi^* = (p^*/\rho_0)_x, \tag{6.2}$$

$$\varphi_{xx}^* = -2\mathscr{R}\rho_0(2+\mathscr{G})\,u^*, \tag{6.3}$$

$$p_z^* = (1/\mathscr{R})\,w_{xx}^*, \tag{6.4}$$

$$H_{xx}^* = 0. \tag{6.5}$$

As the flow is now two-dimensional a formal stream function may then be defined:

$$\rho_0 u^* = -\psi_z, \quad \rho_0 w^* = -\psi_x,$$

and by substituting these quantities in the governing system we obtain

$$\varphi_{xx}^* = 2\mathscr{R}(2+\mathscr{G})\,\psi_z \tag{6.6}$$

and $$\varphi_z^* = -(1/\mathscr{R})\,(\mathrm{e}^x(\mathrm{e}^x\psi_x)_{xx})_x. \tag{6.7}$$

Equations (6.5), (6.6) and (6.7) govern the system and either φ^* or ψ may be eliminated between the latter two. We eliminate φ^* in favour of ψ which yields

$$(\mathrm{e}^x(\mathrm{e}^x\psi_x)_{xx})_{xxx} + 2\mathscr{R}^2(2+\mathscr{G})\,\psi_{zz} = 0.$$

Onsager adroitly introduced a master potential

$$\chi_x = -\psi,$$

thereby obtaining, after integration in x, an equation

$$(\mathrm{e}^x(\mathrm{e}^x\chi_{xx})_{xx})_{xx} + 2\mathscr{R}^2(2+\mathscr{G})\,\chi_{zz} = 0, \tag{6.8}$$

which for flows generated by prescribed conditions on the endcaps yields (through separation of variables) an eigenvalue problem in the radial variable (see subsequent discussion of homogeneous radial conditions). We seek solutions to (6.8) of the form

$$\chi(x,z) = f(x)\,g(z). \tag{6.9}$$

Inserting (6.9) into (6.8) leads to two equations:

$$-(\mathrm{e}^x(\mathrm{e}^x f_{xx})_{xx})_{xx} = \lambda^2 f \tag{6.10}$$

and $$2\mathscr{R}^2(2+\mathscr{G})\,g_{zz} = \lambda^2 g \tag{6.11}$$

where λ^2 is the separation constant.

We shall frequently refer to various differential operators and we choose to simplify notation by establishing the following definitions

$$\mathrm{L}_6 f(x) = [\mathrm{e}^x(\mathrm{e}^x f_{xx})_{xx}]_{xx}, \quad \mathrm{L}_3 f(x) = [\mathrm{e}^x f_{xx}]_x,$$
$$\mathrm{L}_4 f(x) = [\mathrm{e}^x f_{xx}]_{xx}, \quad \mathrm{L}_5 f(x) = [\mathrm{e}^x(\mathrm{e}^x f_{xx})_{xx}]_x.$$

At the rotor wall the conditions on the radial, axial and azimuthal velocities and perturbation temperature can be conveniently expressed in terms of χ (see Wood & Morton 1980), and hence the radial potential function f, as

$$f_x(0) = f_{xx}(0) = \mathrm{L}_5 f(0) = 0. \tag{6.12}$$

The appropriate conditions at $x = x_\mathrm{T}$, $\varphi^*_x = p^* = w^*_x = 0$, may be expressed in terms of the potential function as:

$$f(x_\mathrm{T}) = \mathrm{L}_4 f(x_\mathrm{T}) = \mathrm{L}_3 f(x_\mathrm{T}) = 0. \tag{6.13}$$

The boundary conditions defined above constitute adjoint boundary conditions for L_6 and the eigenvalue problem can be shown to be self-adjoint. In fact pancake theory was originated by Onsager based on a variational principle corresponding to the minimization of a dissipation function.

The endwall boundary conditions are derived by matching to the Ekman layers. As shown in §4, with consistent Ekman-layer expansions, and for mass flow through the endcaps, in the asymptotic limit ($\delta \to 0$) to order $\delta^{\frac{1}{2}}$

$$w^*(x, 0) = W_0(x) \quad \text{and} \quad w^*(x, z_0) = W_{z_0}(x),$$

where $W_0(x)$ and $W_{z_0}(x)$ are prescribed conditions on the axial velocity at the endcaps (note that $z_0 = z_\mathrm{T}/a$). Following Wood & Morton (1980) who numerically generated the axisymmetric eigenfunctions $\{f_k\}$, one may expand the boundary data in terms of the orthonormal set $\{f_k(x)\}$, thereby establishing a solution by eigenvalue expansion.

Solutions for all remaining flow variables may be obtained by solving (6.5) subject to appropriate boundary conditions (see Wood & Morton 1980 for details).

7. Approximate solutions for the non-axisymmetric pancake layer

7.1. *Governing equations*

If we retain the non-axisymmetric terms in (3.7)–(3.11) the system corresponding to the pancake approximation may be obtained into a single sixth-order partial differential equation in terms of w^*. To this end, from (3.8) and (3.10) we obtain

$$\varphi^*_z = (w^*_{xx}/\mathscr{R}\rho_0)_x. \tag{7.1}$$

On eliminating p^* from (3.9) by (3.10) and substituting (3.7) we get

$$\begin{aligned} \varphi^*_{zxxx} &= -2w^*_{xxx\theta} - 2\mathscr{R}\rho_0(H^* - \varphi^*)_{\theta z} - 2\mathscr{R}(2+\mathscr{G})\rho_0 w^*_{zz} \\ &= -2w^*_{xxx\theta} - 2\mathscr{R}\rho_0 H^*_{\theta z} + 2\mathscr{R}\rho_0(w^*_{xx}/\mathscr{R}\rho_0)_{x\theta} - 2\mathscr{R}(2+\mathscr{G})\rho_0 w^*_{zz} \end{aligned}$$

or

$$\varphi^*_{zxxx} = 2w^*_{xx\theta} - 2\mathscr{R}(2+\mathscr{G})\rho_0 w^*_{zz} - 2\rho_0[H^*_z - \mathscr{G}w^*_\theta]_\theta - 2\mathscr{G}\mathscr{R}\rho_0 w^*_{\theta\theta}. \tag{7.2}$$

We may express $[H^*_z - \mathscr{G}w^*_\theta]$ explicitly by combining (3.10) and (3.11), thereby eliminating the pressure terms. This yields

$$[H^*_z - \mathscr{G}w^*_\theta]_{xx} = 0. \tag{7.3}$$

We repeat here that although the range of the stretched coordinate x is typically taken to be infinite in extent, for convenience we shall consider the interval $0 \leqslant x \leqslant x_\mathrm{T}$ where x_T is chosen large enough to simulate the flow accurately as $x \to \infty$.

Equation (7.3) may then be integrated once, employing boundary conditions at the 'top of the atmosphere', (3.14). Carrying out this integration yields

$$[H_z^* - \mathscr{G} w_\theta^*]_x = 0.$$

Upon integrating again and applying boundary conditions at the radial wall ($v^* = w^* = T^* = 0$ at $x = 0$) we find that

$$H_z^* - \mathscr{G} w_\theta^* = 0. \tag{7.4}$$

Finally, combining (7.1), (7.2), and (7.4) we obtain

$$\frac{1}{\rho_0}\left(\frac{1}{\rho_0} w_{xx}^*\right)_{xxxx} - \frac{2\mathscr{R}}{\rho_0} w_{xx\theta}^* + 2\mathscr{R}^2(2+\mathscr{G})\, w_{zz}^* + 2\mathscr{R}^2 \mathscr{G} w_{\theta\theta}^* = 0. \tag{7.5}$$

It is interesting to note that one may take an alternative approach in deriving the governing equation for non-axisymmetric pancake theory. In doing so one obtains a single sixth-order partial differential equation in the perturbation temperature

$$(\mathrm{e}^x(\mathrm{e}^x T_{xxx}^*)_{xx})_x + 2\mathscr{R}^2 \mathscr{G} T_{\theta\theta}^* - 2\mathscr{R}\, \mathrm{e}^x T_{xx\theta}^* + 2\mathscr{R}^2(2+\mathscr{G})\, T_{zz}^* = 0, \tag{7.6}$$

where if we neglect the cross-derivative term we obtain the equation describing flow in the sidewall $E^{\frac{1}{3}}$ thermal layer as described by Matsuda & Nakagawa (1983).

7.2. *Derivation of a non-axisymmetric potential equation*

The problem defined by (7.5) is of sufficient complexity to preclude the application of elementary analytical methods (note that the corresponding differential operator is non-symmetric and contains both even and odd derivatives in θ while solutions must satisfy homogeneous boundary conditions at the θ = constant walls). In lieu of a direct numerical treatment we shall instead make use of previously obtained axisymmetric solutions (see Wood & Morton 1980) in generating solutions which satisfy (7.5). By analogy with the axisymmetric problem (see Wood & Morton 1980), we posit the existence of a non-axisymmetric potential function, χ, such that

$$w^* = \mathrm{e}^x \chi_{xx},$$

which yields

$$(\mathrm{e}^x(\mathrm{e}^x \chi_{xx})_{xx})_{xx} + 2\mathscr{R}^2 \mathscr{G} \chi_{\theta\theta} + 2\mathscr{R}^2(2+\mathscr{G})\, \chi_{zz} - 2\mathscr{R}\, \mathrm{e}^x \chi_{xx\theta} = 0, \tag{7.7}$$

where this equation is obtained by integrating (7.5) twice with respect to x and the functions of integration have been set to zero with no loss of generality (keeping in mind our objective of predicting w^*). Using (3.1)–(3.11) we may express (albeit in axial derivative form) all other variables in terms of χ:

$$p_z^* = \frac{1}{\mathscr{R}} \mathrm{L}_4 \chi, \quad \varphi_z^* = \frac{1}{\mathscr{R}} \mathrm{L}_5 \chi, \quad H_z^* = \mathscr{G}\, \mathrm{e}^x \chi_{xx\theta},$$

$$v_z^* = \frac{1}{\mathscr{G}+2}\left[\mathscr{G} \mathrm{e}^x \chi_{xx\theta} - \frac{1}{\mathscr{R}} \mathrm{L}_5 \chi\right], \quad T_z^* = \frac{1}{\mathscr{G}+2}\left[\frac{\mathscr{G}}{\mathscr{R}} \mathrm{L}_5 \chi + 2\mathscr{G}\, \mathrm{e}^x \chi_{xx\theta}\right],$$

$$\rho_z^* = \frac{1}{\mathscr{R}} \mathrm{L}_4 \chi - \frac{\rho_0}{\mathscr{G}+2}\left[\frac{\mathscr{G}}{\mathscr{R}} \mathrm{L}_5 \chi + 2\mathscr{G}\, \mathrm{e}^x \chi_{xx\theta}\right]$$

and

$$\rho_0 u_z^* = \int_0^x \left\{\frac{\rho^0}{\mathscr{G}+2}\left[\mathscr{G}\, \mathrm{e}^x \chi_{xx\theta\theta} - \frac{1}{\mathscr{R}} \mathrm{L}_5 \chi_\theta + \chi_{xxzz}\right]\right\} \mathrm{d}x,$$

where the conditions on the pancake variables at the bottom endcap ($z = 0$) provide an integral representation for the entire flow field.

For the case of a zero-temperature peripheral wall and zero pressure at the 'top of the atmosphere' the radial boundary conditions on the physical variables ((3.12)–(3.14)) may be shown to be compatible with (6.12) and (6.13) (see Wood & Babarsky 1987). Hence, we impose the following radial conditions on the non-symmetric potential χ:

$$\chi_x(0,\theta,z) = \chi_{xx}(0,\theta,z) = \mathrm{L}_5\chi(0,\theta,z) = 0 \tag{7.8}$$

and

$$\chi(x_\mathrm{T},\theta,z) = \mathrm{L}_3\chi(x_\mathrm{T},\theta,z) = \mathrm{L}_4\chi(x_\mathrm{T},\theta,z) = 0. \tag{7.9}$$

Now in order for the Ekman-layer analysis to be consistent with the case that the interior axial flow is described by (7.1) (and appropriate boundary conditions) we must determine conditions on the interior flow that may be expressed in terms of the axial velocity, w^* (and hence χ). To this end we have, to order $\delta^{\frac{1}{2}}$,

$$W_0(x,\theta) = w^*(x,\theta,0) = \mathrm{e}^x\chi_{xx}(x,\theta,0)$$

and

$$W_{z_0}(x,\theta) = w^*(x,\theta,z_0) = \mathrm{e}^x\chi_{xx}(x,\theta,z_0).$$

In addition, we may use prescribed temperature data to obtain the following condition. From (7.4) we have

$$H^*_z = \mathscr{G}w^*_\theta = \mathscr{G}\,\mathrm{e}^x\chi_{xx\theta},$$

which yields

$$H^*(x,\theta,z_0) - H^*(x,\theta,0) = \mathscr{G}\int_0^{z_0}\mathrm{e}^x\chi_{xx\theta}\,\mathrm{d}z.$$

Applying the matching conditions (4.8) at the top and bottom boundaries we have

$$T_{z_0}(x,\theta) - T_0(x,\theta) = \mathscr{G}\int_0^{z_0}\mathrm{e}^x\chi_{xx\theta}\,\mathrm{d}z, \tag{7.10}$$

where T_{z_0} and T_0 are the temperatures of the top and bottom endcap respectively. We see then that one may provide meaningful conditions at the top and bottom boundaries for the inner axial flow solution by prescribing either mass flow or the temperature differential between the bottom and top endcap.

Analysis of the buoyancy layer implied that the inner flow axial velocity w^* match the prescribed condition on the radial walls. This result may be immediately translated into homogeneous boundary conditions in the θ-variable, to be satisfied by the inner flow solution, i.e. $w^* = 0$ at $\theta = 0$ and $\theta = \theta_0$.

Thus for the azimuthal boundary condition we have

$$\chi_{xx}(x,0,z) = \chi_{xx}(x,\theta_0,z) = 0.$$

Consequently the inner axial flow problem has been completely specified.

One may observe that the axisymmetric pancake operator (6.8) is embedded in (7.7). This suggests a possible approach whereby we seek an approximate solution (to the non-axisymmetric pancake equation) which exhibits the radial characteristics of the axisymmetric solution. We do so by assuming exponential behaviour in the axial variable and constructing a Galerkin-type solution to (7.7) in which we employ basis functions that contain the axisymmetric pancake eigenfunctions $f_k(x)$ as radial factors.

We proceed by seeking solutions to (7.7) of the form

$$\chi(x,\theta,z) = F(x,\theta)H(z). \tag{7.11}$$

Inserting (7.11) into (7.7) leads to two problems – one for F and one for H. These equations are

$$-(\mathrm{e}^x(\mathrm{e}^x F_{xx})_{xx})_{xx} - 2\mathscr{R}^2\mathscr{G}F_{\theta\theta} + 2\mathscr{R}\,\mathrm{e}^x F_{xx\theta} = \lambda F \tag{7.12}$$

and

$$2\mathscr{R}^2(2+\mathscr{G})H_{zz} - \lambda H = 0, \tag{7.13}$$

where λ is the separation constant. Letting $\alpha^2 = \lambda/2\mathscr{R}^2(2+\mathscr{G})$ equation (7.12) becomes

$$H_{zz} - \alpha^2 H = 0,$$

which has solution

$$H = C_1\,\mathrm{e}^{-\alpha z} + C_2\,\mathrm{e}^{\alpha z}.$$

Next we turn our attention to (7.12).

7.3 *Eigenvalue problem*

As a means of obtaining a solution to the non-axisymmetric potential equation we consider the eigenvalue problem

$$\tilde{\mathrm{L}}F = -(\mathrm{e}^x(\mathrm{e}^x F_{xx})_{xx})_{xx} - 2\mathscr{R}^2\mathscr{G}F_{\theta\theta} + 2\mathscr{R}\,\mathrm{e}^x F_{xx\theta} = \lambda F \tag{7.14}$$

for $0 < x < x_{\mathrm{T}}$, $0 < \theta < \theta_0$ subject to the boundary conditions

$$\left.\begin{aligned} F(x_{\mathrm{T}},\theta) = (\mathrm{e}^x F_{xx})_{xx}(x_{\mathrm{T}},\theta) = (\mathrm{e}^x F_{xx})_x(x_{\mathrm{T}},\theta) = 0, \\ F_x(0,\theta) = F_{xx}(0,\theta) = (\mathrm{e}^x(\mathrm{e}^x F_{xx})_{xx})_x(0,\theta) = 0, \\ F(x,0) = F(x,\theta_0) = 0. \end{aligned}\right\} \tag{7.15}$$

In order to achieve continuity in the boundary conditions we have replaced those specified at the θ = constant walls by homogeneous conditions in F.

As discussed above, the problem described by (7.14) and (7.15) lends itself to solution by expansion in terms of the orthonormal functions

$$\phi_i = (2/\theta_0)^{\frac{1}{2}} f_{k_i}(x)\sin(m_i\pi\theta/\theta_0),$$

where the $f_{k_i}(x)$ are the orthonormal eigenfunctions associated with the axisymmetric pancake analysis.

As the familiar energy-related arguments, which are useful in characterizing the solutions to self-adjoint, positive-bounded-below eigenvalue problems are not applicable to the problem defined by (7.14) and (7.15), it might be appropriate to raise questions regarding existence and uniqueness. These questions are considered in the context of operator theory in Babarsky & Wood (1986). The results yield the eigenvalues of (7.14) in conjunction with (7.15) are isolated and form a countable set. Moreover, the corresponding eigenfunctions (and higher-order eigenfunctions) form a complete set in the Hilbert space $\mathscr{H} = \mathscr{L}^2(\boldsymbol{\Omega})$ where $\boldsymbol{\Omega} = (0, x_{\mathrm{T}}) \times (0, \theta_0)$ and the scalar product is given by

$$(u,v) = \int_0^{\theta_0}\int_0^{x_{\mathrm{T}}} u\bar{v}\,\mathrm{d}x\,\mathrm{d}\theta.$$

Furthermore it is shown in Babarsky & Wood (1990) that one may construct a convergent $\perp$-Galerkin method (Chatelin 1983, pp. 170–177) solution to the partial differential equation (7.14) subject to the boundary conditions (7.15), for which the basis functions consists of the orthonormal set $\{\phi_i\} = \{(2/\theta_0)^{\frac{1}{2}} f_{k_i}(x)\sin(m_i\pi\theta/\theta_0)\}$. In

Diameter (m)	—	0.2	—
Reference temperature (K)	—	320	—
Wall pressure p_w (torr)	—	50	—
Wall speed (m/s)	900	1000	1100
Corresponding speed parameter $2A^2$	107	132	160
Ekman number (inverse of the wall Reynolds number) $\times 10^7$	2.36	2.12	1.94
Corresponding value of $\mathscr{R} = \delta^3/E$	3.43	2.02	1.25
Corresponding value of $\mathscr{G} = \Gamma$	3.48	4.29	5.21

TABLE 1. High-speed centrifuge parameters and corresponding values of $\mathscr{R}$ and $\mathscr{G}$ for UF_6

other words, we may obtain a convergent sequence of approximate solutions by solving the $N \times N$ matrix eigenvalue problem

$$\tilde{\mathrm{L}} u_N = \lambda u_N$$

where u_N, the approximate solutions, is assumed to be a linear combination:

$$u_N = \sum_{m=1}^{N} \alpha_m \phi_m.$$

For convenience we split $\tilde{\mathrm{L}}$ into a symmetric part

$$\mathrm{L}F = -(\mathrm{e}^x(\mathrm{e}^x F_{xx})_{xx})_{xx} - 2\mathscr{R}^2 \mathscr{G} F_{\theta\theta}$$

and a non-symmetric part

$$\mathrm{B}F = 2\mathscr{R}\,\mathrm{e}^x F_{xx\theta}.$$

Then the coefficients α_m are determined from the system of algebraic equations

$$\sum_{k=1}^{N} \{(\tilde{\mathrm{L}}\phi_k, \phi_m)\alpha_k - \lambda \delta_{mk} \alpha_k\} = 0, \quad m = 1, 2, \ldots, N$$

or expanding $\tilde{\mathrm{L}}$ we have

$$\alpha_m(\mu_m - \lambda) + \sum_{k=1}^{\infty} \alpha_k(\mathrm{B}\phi_k, \phi_m) = 0, \quad m = 1, \ldots, N \tag{7.16}$$

where μ_m is the ith eigenvalue of L (note that ϕ_m is the corresponding orthonormal eigenfunction). A characteristic value $\lambda = \lambda_N$ of (7.16) satisfies

$$\det[(\mathrm{B}\phi_j, \phi_i) + (\mu_i - \lambda)\delta_{ij}]_{i,j}^{N} = 0$$

and will be taken as an approximate eigenvalue of (7.14); the corresponding approximate eigenvector u_N is defined by the system (7.16) with λ_n substituted for λ.

7.4. *Numerical calculations of eigenelements*

In this section we wish to discuss results of numerical computations for the approximate eigenvalues and eigenfunctions of $\tilde{\mathrm{L}}$. Since $\mathscr{R}$ and $\mathscr{G}$ appear explicitly in the expression for $\tilde{\mathrm{L}}$, the eigenelements will clearly depend on these values. To provide a flavour of the range of parameters within which this analysis is valid (recall that $\mathscr{R} \approx \mathscr{G} \approx 1$ defines non-axisymmetric pancake flow), we shall calculate values of

$\mathscr{R}$ and $\mathscr{G}$ for a centrifuge containing UF_6 which is spinning at several different peripheral speeds. The numerical values associated with a representative geometry and set of operating conditions, along with the corresponding magnitudes of $\mathscr{R}$ and $\mathscr{G}$, are given in table 1. The former are taken from the GSR Rome Machine Model (see Scuricini 1979) centrifuge parameters, with the only difference being the wall pressure, which is one half the minimum value given for the Rome model. We proceed with calculations for the case of $V_{\text{periph}} = 1000$ m/s (along with the operating parameters listed in table 1). This corresponds to $\mathscr{R} = 2.02$ and $\mathscr{G} = 4.29$. In addition, we take $\theta_0 = \frac{1}{3}\pi$ and $x_T = 14.95$, where the latter choice is consistent with the criterion for choosing an inner boundary location as developed by Cooper & Morton (1988). These authors' analysis, in which wave motions in a rotating gas were considered, demonstrated the insensitivity of solutions to the location of the inner boundary provided $x_T > 12$.

As explained above, we obtain approximate solutions by solving the $N \times N$ matrix eigenvalue problem

$$\alpha_m(\mu_m - \lambda) + \sum_{k=1}^{N} \alpha_k(\mathrm{B}\phi_k, \phi_m) = 0, \quad m = 1, \ldots, N$$

The matrix elements $(\mathrm{B}\phi_k, \phi_m)$ are easily obtained by numerical integration utilizing the axisymmetric pancake eigenfunctions $f_k(x)$ and second derivatives $f_{k_{xx}}(x)$ which were generated by Wood & Morton (1980). Although these solutions were obtained for an infinite radial interval the error in using these functions is of order $\mathrm{e}^{-14.95}$.

Calculating the eigenvalues and eigenfunctions of this matrix can be accomplished via a series of well-known EISPACK routines which apply similarity transforms to balance, to reduce to Hessenberg form, and finally to triangularize the matrix.

The result of these eigenvalue calculations are described in detail by Babarsky & Wood (1990). In addition to obtaining the first 40 eigenvalue–eigenfunction pairs for $\tilde{\mathrm{L}}$, the question of the effect of radial ($\theta = \text{const.}$) walls upon the strength of end-driven flows in a gas centrifuge is addressed by considering the notion of decay length. Now, owing to the completeness of the eigenfunctions, the general motion within the centrifuge corresponds to a sum of solutions of (7.14). Letting λ_n and F_n be corresponding eigenvalue–eigenfunction pairs and recalling that $\lambda_n = \alpha_n^2 2\mathscr{R}^2(2+\mathscr{G})$ we can write the general solution for χ as

$$\chi = \sum_{n=1}^{\infty} (A_n F_n(x,\theta)\,\mathrm{e}^{-\alpha_n z} + B_n F_n(x,\theta)\,\mathrm{e}^{-\alpha_n(z_0 - z)}).$$

Physically $1/\mathrm{Re}\,(\alpha_n)$ represents the decay length of the nth mode. That is, if $A_k = 1$ and all other A and B are zero, then the kth mode will be reduced in amplitude by a factor of $1/\mathrm{e}$ in a distance $1/\mathrm{Re}\,(\alpha_k)$. Thus the eigenfunction associated with the lowest value of $\mathrm{Re}\,(\alpha_n)$ corresponds to the kind of motion which extends farthest up (or down) the cylinder.

For the lower modes results suggest that the non-axisymmetric eigenfunctions may be closely identified with a particular two-dimensional, symmetric eigenfunction, ϕ_j (see Babarsky & Wood 1990). In other words, in the Nth approximate Galerkin eigensolution associated with a given (say nth) mode

$$\left(\text{i.e.}\, F^n = \sum_{i=1}^{N} \alpha_i^n \phi_i\right)$$

Mode	α_n^{-1} (axisymmetric)	α_n^{-1} (non-axisymmetric)
1	2.9717	0.38223
2	0.47439	0.29917
3	0.16147	0.14891
4	0.07375	0.07242

TABLE 2. Decay lengths for the first four axisymmetric modes and corresponding non-axisymmetric modes

there is a specific j such that

$$|\alpha_j^n| \approx 1 \quad \text{and} \quad |\alpha_j^n| \gg |\alpha_i^n| \quad \text{for} \quad j \neq i.$$

Hence a comparison of the intensification (or diminishment) of the tendency of the motion within the centrifuge to decay with the introduction of radial walls is most appropriately based on the comparison between the decay lengths of the non-axisymmetric mode corresponding to the symmetric eigenfunction $(2/\theta_0)^{\frac{1}{2}} f_k(x) \sin \theta\pi/\theta_0$ and that of the axisymmetric mode associated with $f_k(x)$. In going from one dimension to two dimensions the characteristic motion associated with the eigenfunction $f_k(x)$ has in a sense been distributed over a countably infinite number of possible motions (i.e. $(2/\theta_0)^{\frac{1}{2}} f_k(x) \sin(m\pi\theta/\theta_0)$, $m = 1, 2, \ldots$) with the most important motion corresponding to the basic mode, $f_k(x) \sin \pi\theta/\theta_0$.

A comparison (on the basis described above) of the decay lengths corresponding to the first four modes is presented in table 2 (the axisymmetric values are taken from Wood & Morton 1980). The motion associated with the fundamental mode (i.e. that mode characterized by the longest decay length) is the most important kind of motion for the action of a high-speed centrifuge. Thus, we see that, for the parameters chosen, the presence of radial walls significantly impedes the resulting non-axisymmetric motions. In other words, for the same set of parameters, axisymmetric motions penetrate significantly farther into the interior of the cylinder than the corresponding non-axisymmetric motions. As for the higher modes, the corresponding eigenfunctions are characterized by increasingly rapid oscillations in the radial coordinate and are associated with motions which are, to a greater degree, influenced (i.e. retarded) by the radial boundaries. Consequently, they are less affected by the presence of the θ = constant walls. This tendency is reflected for these higher modes in the increasingly close agreement between the decay lengths for the axisymmetric and non-axisymmetric cases.

7.5. *Connection with the non-axisymmetric pancake solution*

We now demonstrate that a solution to the potential equation (7.7), i.e.

$$\chi(x, \theta, z) = F(x, \theta) H(z),$$

where $F(x, \theta)$ is an eigenfunction of (7.14) (i.e. a limiting Galerkin solution) and $H(z)$ is a solution to (7.13), satisfies the non-axisymmetric pancake problem, as defined by (7.5)

Now, in Babarsky (1986) the homogeneous radial conditions are shown to be satisfied in the sense of the natural norm of $\mathscr{L}^2(0, \theta_0)$ and the homogeneous azimuthal conditions are shown to be satisfied in the sense of the natural norm of $\mathscr{L}^2(0, x_T)$ by

the limiting Galerkin solution. We next consider the matching conditions. It has been shown in Babarsky & Wood (1986) that the set of eigenfunctions (and higher-order eigenfunctions if they exist) are complete in $\mathscr{H}$; that is, the class of all finite linear combinations of them are dense in $\mathscr{H}$. Thus we may express conditions that the flow is described by the non-axisymmetric potential model as follows: given any $\epsilon > 0$, for N sufficiently large we can find coefficients A_n and B_n $(n = 1, 2, 3, \ldots, N)$ in the approximate expression for the general solution χ, i.e.

$$\chi_N = \sum_{n=1}^{N} (\mathrm{A}_n F_n(x,\theta)\,\mathrm{e}^{-\alpha_n z} + B_N F_n(x,\theta)\,\mathrm{e}^{-\alpha_n(z_0-z)}) \tag{7.17}$$

such that
$$\left\| \mathscr{B}_1(x,\theta) - \sum_{n=1}^{N} (A_n + B_n\,\mathrm{e}^{-\alpha_n z_0}) F_n(x,\theta) \right\| < \epsilon \tag{7.18}$$

and
$$\left\| \mathscr{B}_2(x,\theta) - \sum_{n=1}^{N} (A_n\,\mathrm{e}^{-\alpha_n z_0} + B_n) F_n(x,\theta) \right\| < \epsilon, \tag{7.19}$$

where, if mass flow data are prescribed,

$$\mathscr{B}_1(x,\theta) = \int_0^x \int_0^{x'} \rho_0 W_0(x'',\theta)\,\mathrm{d}x''\,\mathrm{d}x' \quad \text{and} \quad \mathscr{B}_2(x,\theta) = \int_0^x \int_0^{x'} \rho_0 W_{z_0}(x'',\theta)\,\mathrm{d}x''\,\mathrm{d}x',$$

and if temperature data are prescribed,

$$\left\| \mathscr{B}(x,\theta) - \sum_{n=1}^{\infty} ((1-\mathrm{e}^{-\alpha_n z_0})/\alpha_n)(A_n + B_n) F_n(x,\theta) \right\| < \epsilon,$$

where
$$\mathscr{B}(x,\theta) = \int_0^x \int_0^{x'} \int_0^{\theta'} [T_{z_0}(x'',\theta') - T_0(x'',\theta)]\,\mathrm{d}\theta'\,\mathrm{d}x''\,\mathrm{d}x'.$$

For computational purposes, however, we shall consider consistent approximations for the matching equations. Substituting (7.17) for χ in these equations yields for the mass flow case

$$\sum_{n=1}^{\infty} A_n F_{n_{xz}}(x,\theta) + \sum_{n=1}^{\infty} B_n\,\mathrm{e}^{-\alpha_n z_0} F_{n_{xz}}(x,\theta) = \rho_0 W_0(x,\theta), \tag{7.20}$$

$$\sum_{n=1}^{\alpha} A_n\,\mathrm{e}^{-\alpha_n z_0} F_{n_{xz}}(x,\theta) + \sum_{n=1}^{\infty} B_n F_{n_{xz}}(x,\theta) = \rho_0 W_{z_0}(x,\theta), \tag{7.21}$$

and for the temperature differential case

$$\sum_{n=1}^{\infty} ((1-\mathrm{e}^{-\alpha_n z_0})/\alpha_n)(A_n + B_n) F_{n_{xz\theta}}(x,\theta) = T_{z_0}(x,\theta) - T_0(x,\theta). \tag{7.22}$$

It is in this sense that the end conditions are satisfied. This completes the consideration of the boundary conditions.

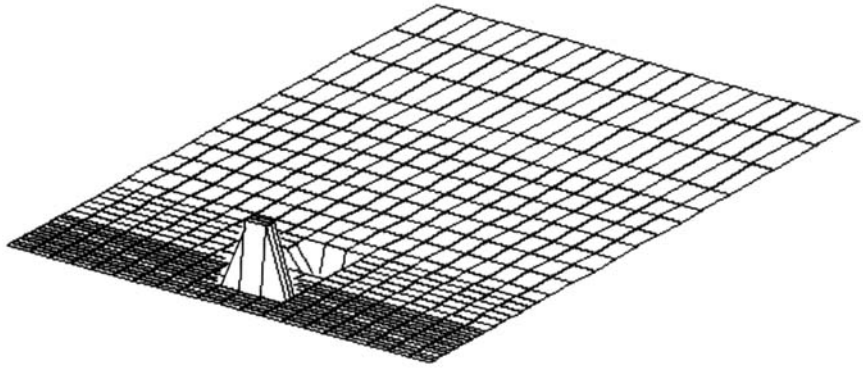

FIGURE 4. Boundary condition for axial mass flux (values range from -0.5 to 1.0).

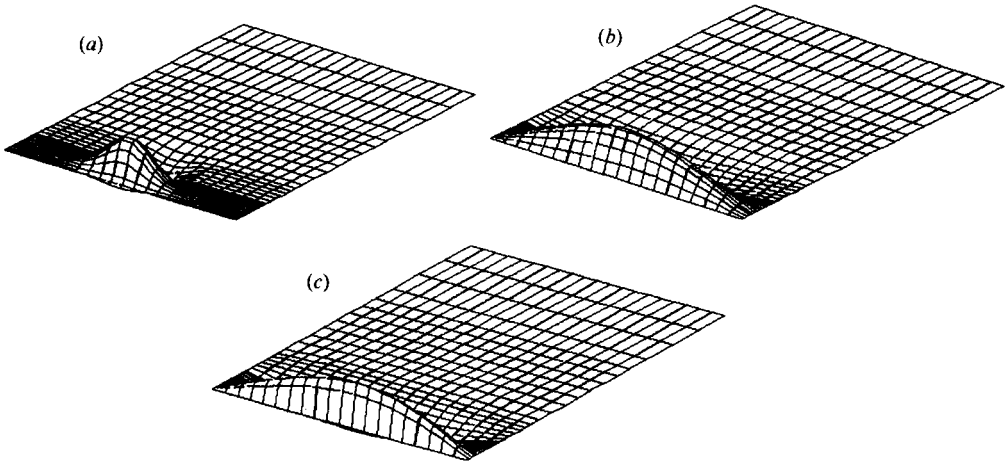

FIGURE 5. Axial mass flux for flow driven by an axial mass flux through endcaps at: (a) $\frac{1}{64}z_0$ (values range from -0.322 to 0.656); (b) $\frac{1}{8}z_0$ (values range from -0.0345 to 0.0714789); (c) $\frac{1}{2}z_0$ (values range from -0.000508 to 0.000145).

8. Results

In this section we present results of numerical computations for two simple choices of boundary data. In addition to the parameter values indicated above, we take $z_0 = 2.5$.

Approximate solutions were obtained by truncating the infinite series (7.17) after 40 terms and evaluating the left-hand sides of (7.20) and (7.21) or (7.22) at a number of points in the (x, θ)-plane. (These calculations were performed using a mesh of 24 radial grid points and 15 azimuthal grid points.) The coefficients A_n and B_n, $n = 1, 2, 3, \ldots,$ 40, can then be determined by linear least squares. It should be noted that in both cases treated below the mass conservation constraint gives rise to axial flows which are symmetric about the midplane ($z = \frac{1}{2}z_0$), hence, A_n and B_n are equal for each n.

In the first case considered, the countercurrent flow is induced by introducing and removing mass through the endcaps. In particular, on the bottom endcap a uniform mass flux of unit amplitude is introduced in the region $(0.75 \leqslant x \leqslant 1.25$, $0.45\theta_0 \leqslant \theta \leqslant 0.55\theta_0$ and a uniform mass flux of amplitude 0.5 is removed in the region $(2.5 \leqslant x \leqslant 3.5$; $0.45 \leqslant 0 \leqslant 0.55\theta_0)$. On the top endcap, symmetric conditions

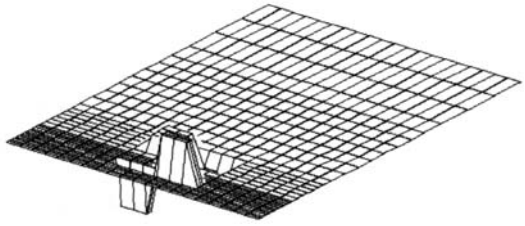

FIGURE 6. Temperature differential condition (values range from -1.0 to 1.0).

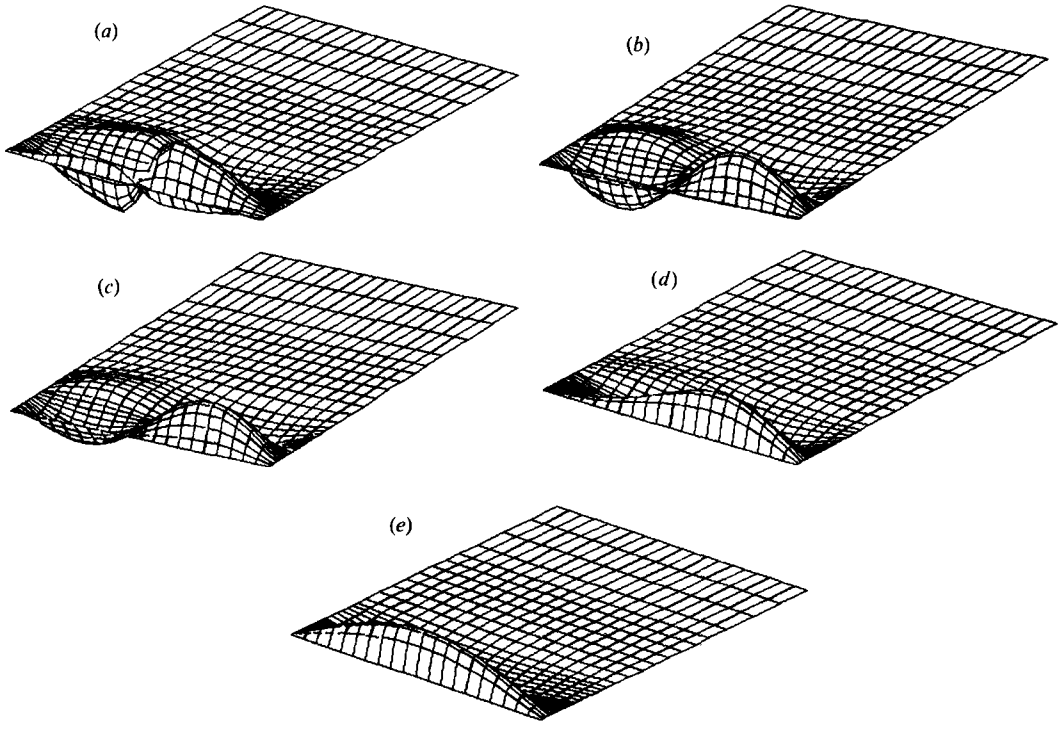

FIGURE 7. Axial mass flux for flow driven by temperature boundary conditions at: (*a*) $\frac{1}{64}z_0$ (values range from 0.0396 to 0.04); (*b*) $\frac{1}{8}z_0$ (values range from -0.000175 to 0.0019); (*c*) $\frac{1}{4}z_0$ (values range from -0.000055 to 0.000087); (*d*) $\frac{3}{8}z_0$ (values range from -0.000004 to 0.0000072); (*e*) $\frac{1}{2}z_0$ (values range from -0.00000154 to 0.00000266).

are imposed with mass removed for $(0.75 \leqslant x \leqslant 1.25,\ 0.45\theta_0 \leqslant \theta \leqslant 0.55\theta_0)$ and introduced for $(2.50 \leqslant x \leqslant 3.50,\ 0.45\theta_0 \leqslant \theta \leqslant 0.55\theta_0)$. The end conditions are depicted in figure 4.

The countercurrent flow is determined by the axial mass flux which is shown in figure 5(*a–c*) as a function of θ and x at the axial locations of $\frac{1}{64}z_0$, $\frac{1}{8}z_0$, and, $\frac{1}{2}z_0$ respectively.

A second case has been considered in which the countercurrent flow is induced by a temperature differential between the two axial boundaries. As an example, on the top endcap, we impose a perturbation temperature distribution of unit magnitude in the region $(0.75 \leqslant x \leqslant 1.25,\ 0.5\theta_0 \leqslant \theta \leqslant 0.55\theta_0)$ and a temperature deficit of 0.5 in the region $(2.5 \leqslant x \leqslant 3.5,\ 0.5\theta_0 \leqslant \theta \leqslant 0.55\theta_0)$. The temperature profile on the bottom endcap is the reflection of that described above with respect to the midplane $\theta = \frac{1}{2}\theta_0$. However, we note that axial asymmetries which arise from the discrepancy between

prescribed temperature conditions at the top and bottom endcaps are mediated through the Ekman layers, the inner axial flow being driven solely by the temperature differential profile. This differential condition is shown in figure 6.

Similar results are presented for this case as were presented for the mass-driven case. Figure 7 (a–e) shows the axial mass flux as a function of x and θ at the axial locations $\frac{1}{64}z_0$, $\frac{1}{8}z_0$, $\frac{1}{4}z_0$, $\frac{3}{8}z_0$, and $\frac{1}{2}z_0$, respectively.

In viewing these figures, one should keep in mind that although the geometry shown is rectangular this simplification results from the neglect of curvature in the high-speed limit being considered. A physically realistic depiction of the flow geometry would not only exhibit curvature but would also reflect the exceedingly small ratio $x_T/\theta_0 a$ where a is the radius of the centrifuge.

As regards the mass-driven and temperature-driven profiles we see that their evolution (in z) exhibits the tendency of the flow to decay to the fundamental eigenmode (that eigenfunction corresponding to the lowest value of $\mathrm{Re}(\alpha_n)$). This property of the axial mass flows is further illustrated by the relative strength of the flow associated with the mass flow boundary condition which excites the fundamental mode to a greater degree than does the thermal condition.

9. Conclusions

A solution technique has been developed for analysing end-driven, compressible flow in a rapidly rotating, pie-shaped, cylinder. Approximate solutions have been obtained for the case of non-homogeneous end conditions corresponding to mass throughput and a temperature differential between endcaps.

Two main conclusions may be drawn concerning the effects of radial walls on the countercurrent flow. The first follows immediately from the fact that the buoyancy-layer contribution for w, the axial velocity, vanishes. This implies that the axial velocity cannot decay sharply near the radial walls, but must fall off gradually, thereby significantly reducing the axial mass flux compared to the open-cylinder case. Secondly, the decay length of the fundamental mode $(1/\alpha_1)$ is significantly shorter than that of the corresponding axisymmetric case. Consequently, end-driven flows must decay quite rapidly with distance away from the axial boundary.

REFERENCES

Babarsky, R. J. 1986 Compressible flow in a pie-shaped cylinder rotating about the vertex. Ph.D. dissertation, School of Engineering and Applied Science, University of Virginia, Charlottesville.

Babarsky, R. J. & Wood, H. G. 1986 On the eigenvalue problem for a certain non-self-adjoint operator. *Stud. Appl. Maths* **75**, 249–264.

Babarsky, R. J. & Wood, H. G. 1990 Approximate eigensolutions for non-axisymmetric, rotating compressible flows. *Comput. Meth. Appl. Mech. Engng* **81**, 317–332.

Chatelin, F. 1983 *Spectral Approximations of Linear Operators*. Academic.

Cooper, G. R. & Morton, J. B. 1988 Driven linear wave motions in a rotating gas. *J. Fluids and Struct.* **2**, 453–477.

Kerkorkian, J. & Cole, J. D. 1981 *Perturbation Methods in Applied Mathematics*. Springer.

Maslen, S. H. 1984 Unsymmetrical flow in a centrifuge. *School of Engineering and Applied Science, University of Virginia, Rep.* UVA-ER-953-84U.

Matsuda, T. & Nakagawa, K. 1983 Anew type of boundary layer in a rapidly rotating gas. *J. Fluid Mech.* **126**, 431–442.

Rätz, E. 1978 *Uranium Isotope Separation in the Gas Centrifuge. Lecture Series 1978, von Kármán Inst. for Fluid Dynamics*, Belgium.

SAKURAI, T. & MATSUDA, T. 1974 Gasdynamics of a centrifuge machine. *J. Fluid Mech.* **62**, 727–736.

SCHLEINIGER, G. F. & COLE, J. D. 1982 An asymptotic study of pancake theory. In *Proc. 4th Workshop on Gases in Strong Rotation, Oxford* (ed. E. Rätz), pp. 678–688. Frankenforster Strasse 21, Bergisch Gladbach 1, Germany.

SCURICINI, D. B. (Ed.) 1979 *Proc. Third Workshop on Gases in Strong Rotation, Rome, Italy.* Comitato Nazionale Energia Nucleare, Viale Regina Margherita 125, Rome, Italy.

SOUBBARAMAYER 1979 Centrifugation. In *Uranium Enrichment* (ed. S. Villani), pp. 183–244. Springer.

WOOD, H. G. & BABARSKY, R. J. 1987 Analysis of geometric effects on rotating compressible flows: Part I. In *Proc. Workshop on Separation Phenomena in Liquids and Gases* (ed. K. G. Roesner & E. Rätz), pp. 530–601. Darmstadt Technische Hochschule, Darmstadt, Germany.

WOOD, H. G. & MORTON, J. B. 1980 Onsager's pancake approximation for the fluid dynamics of a gas centrifuge. *J. Fluid Mech.* **101**, 1–31.